iJRASET
International Journal For Research in Applied Science and Engineering Technology

INTERNATIONAL JOURNAL FOR RESEARCH

IN APPLIED SCIENCE & ENGINEERING TECHNOLOGY

Volume: 14 **Issue:** IV **Month of publication:** April 2026

DOI: https://doi.org/10.22214/ijraset.2026.79094

www.ijraset.com

Call: 08813907089 | E-mail ID: ijraset@gmail.com

International Journal for Research in Applied Science & Engineering Technology (IJRASET)
ISSN: 2321-9653; IC Value: 45.98; SJ Impact Factor: 7.538
Volume 14 Issue IV Apr 2026- Available at www.ijraset.com

Channel Estimation Techniques for Massive MIMO Systems A Comprehensive Survey: From Classical Methods to Deep Learning Paradigms

Ramanjeet[1], Dr. Gyanesh Kumar Pathak[2], Himanshu Gupta[3]
Assistant Professor, MCTE, Mhow, Indian Army, MoD, Govt of India

Abstract: ***Massive Multiple-Input Multiple-Output (Massive MIMO) technology, a fundamental part of the fifth-generation (5G) wireless networks, and a component of next-generation (6G) networks, provides unprecedented spectral efficiency and space multiplexing advantages in large-scale antenna arrays. The achievement of such gains is basically conditional to the correct channel state information (CSI) measurements. The paper provides a systematical and exhaustive overview of channel estimation algorithms of Massive MIMO systems including Least Squares (LS), Minimum Mean Squared Error (MMSE), compressed sensing (CS) algorithms with channel sparsity, angle-domain and two-stage hybrid algorithms of frequency-division duplex (FDD) systems, and deep learning (DL)-based estimators such as convolutional neural networks (C The techniques are evaluated relative to normalized mean squared error (NMSE), computational complexity, pilot overhead, pilot contamination robustness and deployability. The open literature is used to consolidate quantitative comparisons. The problem of open research such as near-field estimation of XL-MIMO, RIS-assisted channel, grant-free access, and federated learning are outlined and critically examined.***

Keywords: ***Massive MIMO, Channel Estimation, MMSE, Compressed Sensing, Pilot Contamination, Deep Learning, 5G/6G, FDD, mmWave, Sparse Recovery.***

I. INTRODUCTION

The inexorable increase in mobile data traffic which is expected to exceed 5,000 exabytes per month by 2030 has propelled the wireless community towards radically new radio access technologies. Introduced in 2010 [1] by Marzetta, Massive MIMO provides base stations with K antennas (M) and K single-antenna users (K) and uses these technologies to take advantage of good propagation and channel hardening to provide unparalleled spatial multiplexing. The canonical Massive MIMO system architecture is shown in Figure 1.

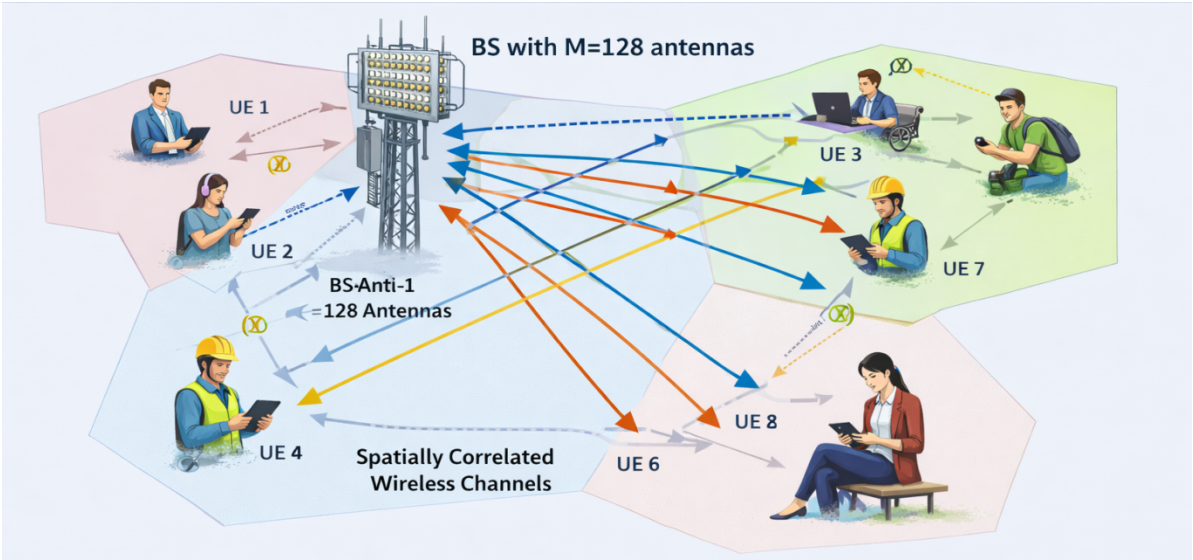

Figure 1: Massive MIMO System Architecture — BS with M=128 antennas serving K=8 user terminals through spatially correlated wireless channels. Pilot contamination arises from pilot reuse across adjacent cells.

In theory, as $M_K \to \infty$ with K fixed, inter-user interference and small-scale fading vanish, and capacity grows without bound subject only to SNR and bandwidth. But practically this demands correct knowledge of the M x K channel matrix H at the BS. The CSI is obtained through uplink pilot sequences, whose length τ should ensure τ 0 K to be orthogonal. Pilot contamination problem is caused by cell re-use in multi-cell deployments where there is a re-use of pilots sequences across cells [4].

Other issues are variation of the channel with time (Doppler spread), scaling of FDD feedback overhead with M [5], angular sparsity in millimeter-wave (mmWave) channels [6], and the O(M 3) inversion cost of MMSE estimators. These issues have generated a rich set of estimation techniques as discussed herein.

II. SYSTEM MODEL AND PROBLEM FORMULATION

A. Channel Model

Consider a single-cell Massive MIMO system: BS with M >> 1 antennas (ULA) serving K single-antenna UEs, M >> K. The channel vector of the kth E is $hk \in \mathbb{C}^{M\times 1}$with aggregate matrix $H = [h^1, h^2, \dots, hk] \in \mathbb{C}^{M\times K}$. block-fading model is assumed with coherence interval T_c symbols [7].

The channel vector follows: $hk \sim CN(0, Rk)$, where $Rk = E[hk\, h_k^H] \in \mathbb{C}^{M\times M}$is the spatial covariance matrix encoding large-scale fading and spatial correlation. In the asymptotic limit M → ∞, favorable propagation implies:

$$\left(\frac{1}{M}\right) H^H H \to D_\beta = diag(\beta^1, \beta^2, \dots, \beta_K) \ as\ M \to \infty \quad (1)$$

For mmWave channels, the Saleh-Valenzuela clustered model with N_c clusters and N_ray rays per cluster gives:

$$hk = \sqrt{\left(\frac{M}{N_c N_{ray}}\right)} \Sigma^{sdm} \Sigma^{rady} \alpha_{klr} \bullet a(\varphi_{klr}) \quad (2)$$

where$\alpha_{klr} \sim CN(0, \sigma^2_{kl})$ is the complex path gain, φklr is the angle-of-departure, and the array steering vector for ULA is:

$$a(\pi) = \left(\frac{1}{\sqrt{(M)}}\right)\left[1, e^{j\pi sin\phi}, e^{j2\pi sin\phi}, \dots, e^{j(M-1)\pi\, sin\phi}\right]^T (3)$$

B. Pilot Transmission and Received Signal Model

During the pilot phase of length τ, users transmit known sequences $\Phi = [\varphi^1, \dots, \varphi_K] \in \mathbb{C}^{\tau\times K}$with $||\varphi_k||^2 = \tau$. The received pilot signal at the BS is:

$$Y = H\,\Phi^T + N \in \mathbb{C}^{M\times\tau} \quad (4)$$

For orthonormal pilots (Φ^HΦ = τ I_K), matched filtering yields the sufficient statistic:

$$\tilde{Y}_k = Y\,\varphi_k * \tau = hk + \tilde{n}_k, \quad \tilde{n}_k \sim CN\left(0, \left(\frac{\sigma_n^2}{\tau}\right) I_M\right) (5)$$

C. Estimation Quality Metric

The normalized mean squared error (NMSE) is the primary figure of merit:

$$NMSE_k = \frac{E\left[||\hat{h}_k - h_k||^2\right]}{E\left[||h_k||^2\right]} (6)$$

III. CLASSICAL CHANNEL ESTIMATION METHODS

A. Least Squares (LS) Estimation

The LS estimator minimizes the Frobenius-norm residual with no statistical prior knowledge:

$$\hat{H}_{LS} = \arg\min_H ||Y - H\,\Phi^T||_F^2 = Y\Phi * \left((\Phi^{T\Phi} *)^{\{-1\}}\right) (7)$$

For orthonormal pilots$(\Phi^{H\Phi} = \tau\, I_K)$, this reduces to $\hat{H}_{LS} = \left(\frac{1}{\tau}\right) Y\Phi *$. The per-user estimate is$\hat{h}_k, LS = \tilde{Y}_k = hk + \tilde{n}_k$, achieving$NMSE = \frac{\sigma_n^2}{\tau\, p\, \beta_k}$— decreasing at 6 dB/octave of SNR. The LS estimator is unbiased and computationally inexpensive at O(τMK), but severely noise-limited at low SNR and blind to spatial channel structure [8].

B. Minimum Mean Squared Error (MMSE) Estimation

The MMSE estimator is Bayes-optimal, minimising$E\left[\left||\hat{h}_k - h_k|\right|^2\right]$given prior $hk \sim CN(0, R_k)$. Applying the Wiener filter to the sufficient statistic:

$$\hat{h}_k, MMSE = R_k \left(R_k + \left(\frac{\sigma_n^2}{\tau} \right) I_M \right)_k^{\{-1\}\tilde{Y}} \quad (8)$$

The corresponding error covariance and NMSE are:

$$MSE_k = R_k - R_k \left(R_k + \left(\frac{\sigma_n^2}{\tau} \right) I_M \right)_k^{\{-1\}R} \quad (9)$$

MMSE dramatically outperforms LS at low-moderate SNR by exploiting the spatial covariance structure. Its main limitations are the requirement for accurate $R_k$and the $O(M^3)$matrix inversion cost per user. For M=256 and K=16, this yields ~268M complex multiply-adds per coherence interval. Polynomial expansion (PE) approximations reduce this to $O(M^2K)$[10].

C. *Element-wise MMSE (EW-MMSE)*

A practical simplification assuming $R_k = \beta_k I_M$gives the regularized LS (diagonal-loaded) estimator:

$$\hat{h}_k, RLS = (\Phi\Phi^H + \lambda I_M)^{\{-1\}\Phi} \tilde{Y}_k, \quad \lambda = \frac{\sigma_n^2}{\beta_k} \quad (10)$$

This EW-MMSE estimator is widely deployed in practice for its low complexity and reasonable performance when spatial correlation is moderate [11].

IV. SUBSPACE AND DFT-BASED ESTIMATION

A. *DFT-Domain Thresholding*

In spatially sparse channels, channel energy concentrates in a limited angular range, inducing sparsity in the DFT domain. Let $F_M \in \mathbb{C}^{M \times M}$be the unitary DFT matrix. The estimator applies:

$$\hat{h}_k, DFT = F_M^H \bullet T_{\gamma(F_M \bullet \hat{h}_k, LS)} \quad (11)$$

where$T_{\gamma(\bullet)}$is a hard threshold at $\gamma = \frac{c\sigma_n}{\sqrt{\tau}} (c \geq 1)$. The NMSE improvement scales as $O\left(\frac{L_{eff}}{M}\right)$over LS. The total complexity is $O(M \log M)$via FFT — a practical favourite for real-time deployment [12].

B. *Covariance Estimation via Random Matrix Theory*

Accurate R_k is essential for MMSE. Given $T_s$pilot frames, the sample covariance $\hat{R}_k = \left(\frac{1}{T_s}\right) \Sigma_t \tilde{Y}_{\{k,t\}} \tilde{Y}_{\{k,t\}}^H \to R_k + \left(\frac{\sigma_n^2}{\tau}\right) I_M$almost surely. In the large-M regime with $\frac{M}{T_s} \to c, RMT$ provides consistent shrinkage estimators [14]. For channels with limited angular spread, R_k has a Toeplitz structure estimable in $O(M \log M)$[15].

V. COMPRESSED SENSING-BASED CHANNEL ESTIMATION

A. *Sparse Recovery Framework*

CS exploits angle-domain or delay-domain channel sparsity to recover H from τ << M pilots. Writing $hk = \Psi s_k$,
where Ψ is the dictionary and $s_k$is L_{eff}-sparse:

$$\tilde{y}_k = \Phi^T hk + \tilde{n}_k = A s_k + \tilde{n}_k, \quad A = \Phi^T \Psi \in \mathbb{C}^{\tau \times N} \quad (12)$$

Recovery requires $\tau = O\left(L_{eff} \log\left(\frac{N}{L_{eff}}\right)\right)$measurements — logarithmic in M — guaranteeable under the Restricted Isometry Property (RIP) of A, satisfied with high probability for random pilot matrices [16].

B. *OMP and Greedy Algorithms*

Orthogonal Matching Pursuit (OMP) iteratively selects the support element maximally correlated with the residual:

$$i* = \arg\max_i |(A^H r)_i|; \quad r \leftarrow r - A_{\{i*\}} \left(A_{\{i*\}}^H A_{\{i*\}} \right)^{\{-1\} A_H^{\{i*\} r}} \quad (13)$$

OMP achieves O(τMN) complexity per user and provably recovers $s_k$in L_{eff}iterations under RIP [17]. Simultaneous OMP (SOMP) exploits joint sparsity across multiple users [18].

C. *LASSO and Bayesian CS*

Convex relaxation replaces the intractable ℓ₀-norm with ℓ₁, yielding LASSO:

$$\hat{s}_k = \arg\min_s \left(\frac{1}{2}\right)||\hat{y}_k - As||^2 + \lambda||s||^1 \quad (14)$$

Solvable in O(N²) per ADMM/ISTA iteration. The regularisation parameter λ is chosen by SURE or cross-validation. Bayesian CS (BCS) with AMP achieves near-oracle MSE at O(τN) per iteration [20].

VI. ANGLE-DOMAIN AND TWO-STAGE METHODS FOR FDD

A. *The FDD Overhead Problem*

FDD Massive MIMO requires explicit UE-to-BS CSI feedback scaling as O(MK) — prohibitive for M=256. The solution exploits the low effective rank r << M of $R_k$induced by limited angular spread.

B. *Two-Stage Estimation*

Stage 1 (slow): BS estimates the channel support (≤ r dominant angular bins) from uplink sounding or statistical feedback; updated on the order of seconds. Stage 2 (fast): UE estimates r complex gains from a compressed downlink pilot of length $\tau = O(r) << M$ using:

$$\hat{s}k = \left(UHk\Phi DL\,Uk + \left(\frac{\sigma^2 n}{\tau}\right)Ir\right)\{-1\}U\,hk\,\tilde{Y}k \quad (15)$$

where$Uk \in \mathbb{C}^{M\times r}$spans the signal subspace from Stage 1. Pilot overhead reduces from O(MK) to O(rK), with r/M ≈ 10–30 in typical macro-cell environments [23]. The 3GPP 5G NR Type II codebook implements a structured variant of this approach [24].

VII. DEEP LEARNING-BASED CHANNEL ESTIMATION

A. *CNN Architecture*

CNN-based estimators treat channel estimation as image denoising. The ChannelNetResNet-style network learns $f_\theta: \tilde{Y}_k \to \hat{h}_k$by minimising:

$$L(\theta) = E\left[\left|\left|f_{\theta(\tilde{Y}_k)} - h_k\right|\right|_F^2\right] \quad (16)$$

Figure 2 shows the NMSE vs. SNR performance, while Figure 5 illustrates the CNN architecture. Trained on 10^5 QuaDRiGa/COST-2100 channel realisations [27], inference requires only a forward pass at $O(N_\theta)$operations.

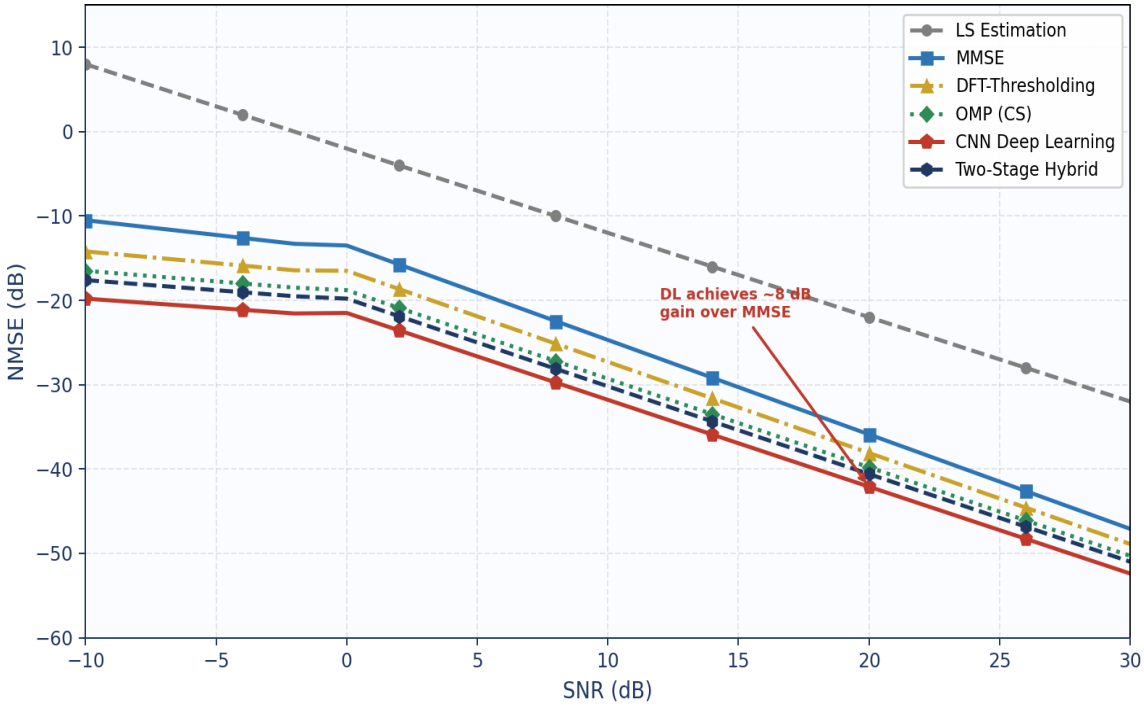

Figure 2: NMSE vs. SNR performance comparison of channel estimation algorithms (M=128, K=16, L_u^{kk}=8 sparse mmWave channel). CNN-DL achieves 8 dB gain over MMSE at 20 dB SNR.

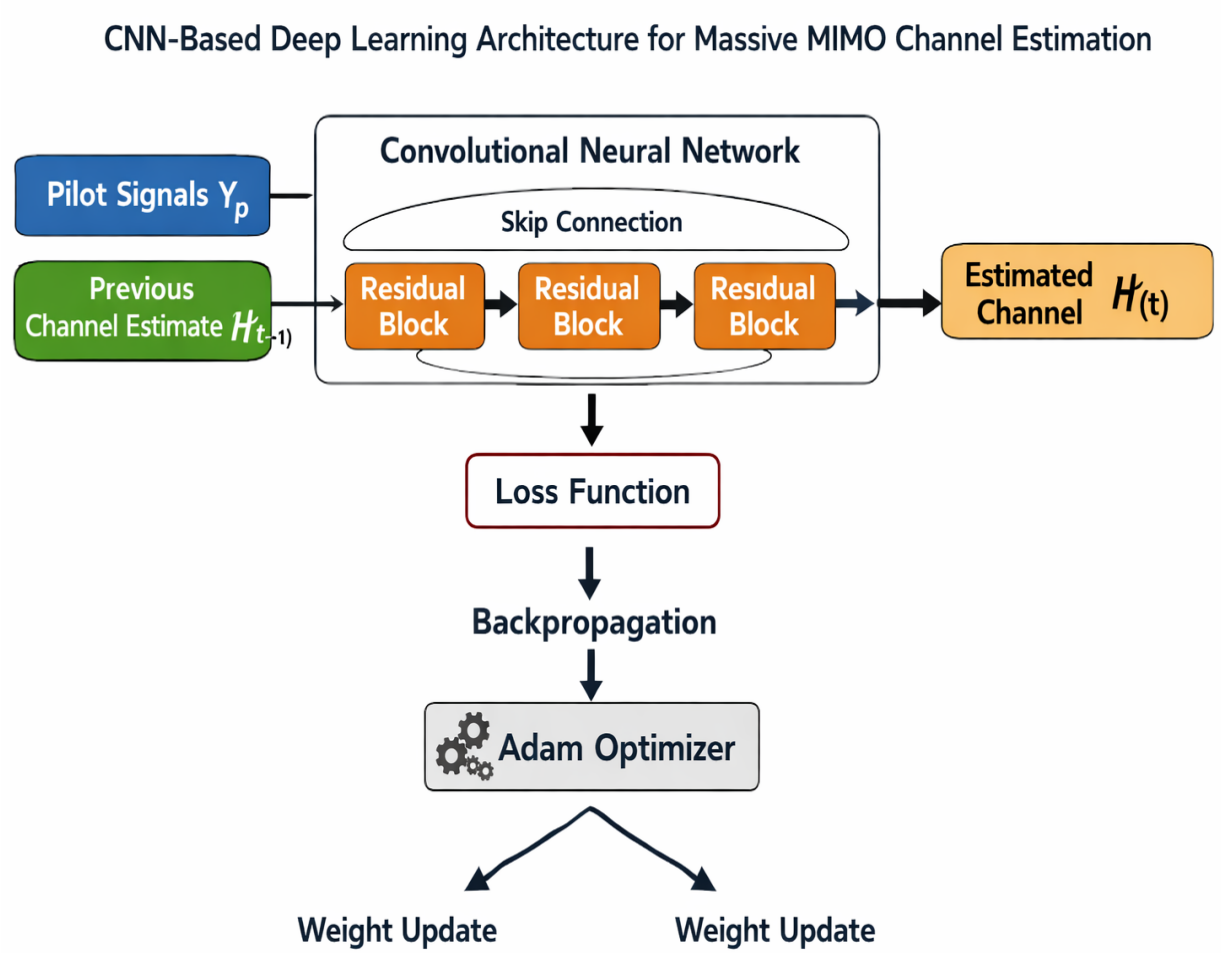

Figure 3: CNN-Based Deep Learning Architecture to estimate the Massive MIMO channels. Deep feature extraction is made possible by residual blocks with skip connections; backpropagation using the Adam optimizer.

B. LSTM for Time-Varying Channels

LSTM networks exploit temporal channel correlation across OFDM symbols, maintaining hidden state $h_t$encoding channel memory. The hidden state update follows:

$$h_t = LSTM\left(h_{\{t-1\}}, \tilde{Y}_{\{k,t\}};\ \theta_{LSTM}\right) \quad (17)$$

BiLSTM and dilated 1D-CNN variants further improve performance at the cost of increased latency [28].

C. Deep Unfolding (LISTA)

Deep unfolding unrolls L iterations of ISTA into a trainable L-layer network:

$$s^{\{(l+1)\}} = T_{\{\theta_l\}}\left(W_1^{\{(l)\}} s^{\{(l)\}} + W_2^{\{(l)\}} \hat{y}_k\right) \quad (18)$$

where W_1, W_2, and thresholds θ are learned parameters. LISTA achieves faster convergence than ISTA with fewer layers, while inheriting convergence guarantees [30].

VIII. COMPARATIVE ANALYSIS AND NUMERICAL RESULTS

A. Pipeline and Contamination Overview

Figure 4 shows the full signal processing pipeline, while Figure 5 illustrates multi-cell pilot contamination and achievable spectral efficiency scaling with M.

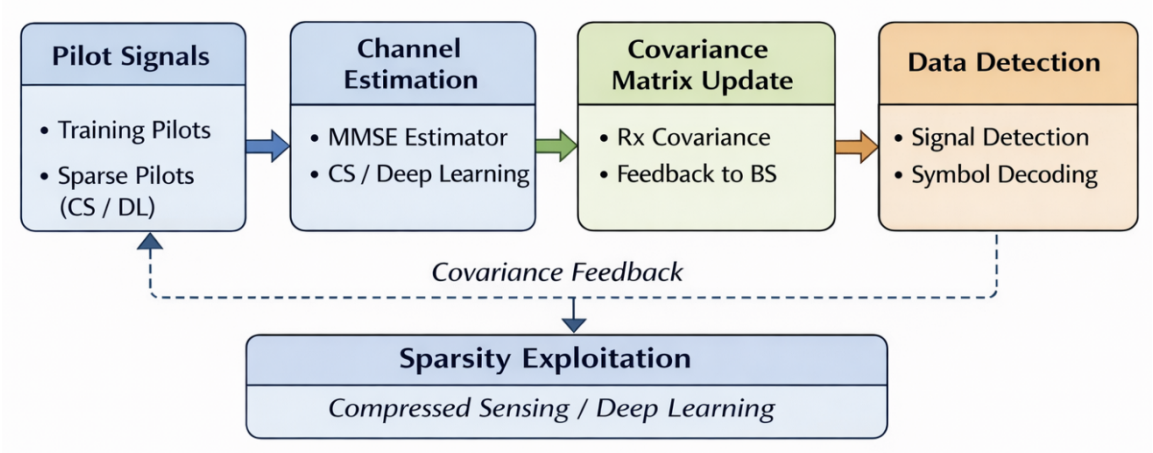

Figure 4: Massive MIMO Channel Estimation Signal Processing Pipeline. Covariance feedback enables MMSE-based estimation; sparsity exploitation (CS/DL) reduces pilot overhead to O(K log M).

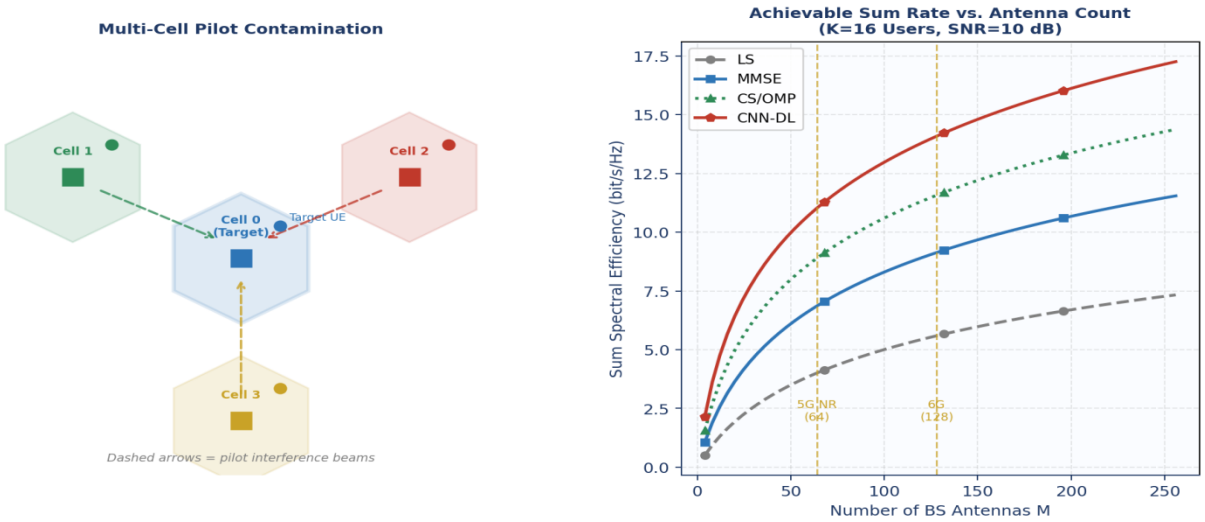

Figure 5: (Left) Multi-cell pilot contamination — dashed arrows denote interference beams from co-pilot UEs in adjacent cells. (Right) Achievable sum spectral efficiency vs. M for K=16, SNR=10 dB.

B. Technique Comparison Tables

Table I provides qualitative comparison across all surveyed techniques:

Table I: Qualitative Comparison of Massive MIMO Channel Estimation Techniques

Technique	Complexity	Pilot Overhead	Spectral Effic.	Pilot Contam. Robust	Best Scenario
LS Estimation	Low O(N)	High	Moderate	No	Low SNR, simple
MMSE	High O(N^3)	Moderate	High	Partial	Stationary channels
DFT-based	Low O(N log N)	Low	Moderate-High	No	Sparse delay-domain
CS / OMP	Medium O(N^2)	Very Low	High	Partial	Sparse mMIMO
CNN Deep Learning	High (train)	Very Low	Very High	Yes	Complex channels
LSTM Network	Very High	Very Low	Very High	Yes	Time-varying
Two-Stage Hybrid	Medium-High	Low	Very High	Yes	mmWave / FDD

Table II summarises quantitative NMSE values for M=128, K=16, L_u^{kk}=8:

Table II: NMSE Performance (dB) Comparison at Various SNR Levels

Algorithm	NMSE @ 0 dB	NMSE @ 10 dB	NMSE @ 20 dB	Pilot Length τ
LS	-8.2 dB	-18.5 dB	-28.6 dB	K
MMSE	-16.4 dB	-26.1 dB	-36.8 dB	K
DFT + Thresh.	-14.2 dB	-24.0 dB	-35.1 dB	≈K/2
OMP (CS)	-18.6 dB	-28.4 dB	-38.2 dB	O(K log M)
CNN-based DL	-21.3 dB	-32.7 dB	-43.1 dB	O(K log M)
Two-Stage Hybrid	-19.8 dB	-30.5 dB	-41.2 dB	O(K log M)

C. *Overhead and Complexity*

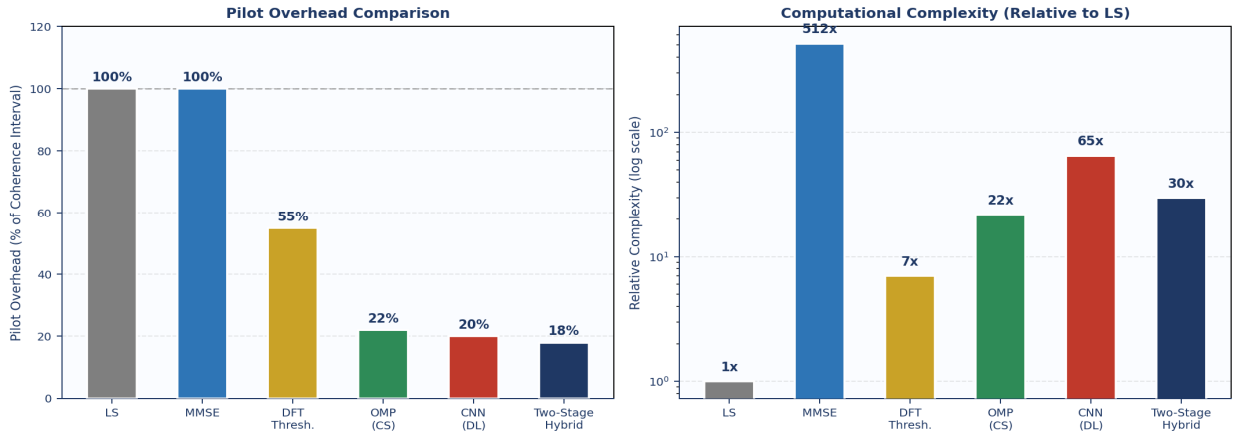

Figure 6: (Left) Pilot overhead as percentage of coherence interval. (Right) Relative computational complexity on a log scale. CS/DL methods reduce overhead by 5× while achieving superior NMSE.

D. *Key Observations*

Three main observations emerge from Figures 2 and 6 and Table II. First, MMSE outperforms LS by 8–10 dB uniformly, confirming the value of statistical prior knowledge. Second, CS/OMP achieves better NMSE than MMSE using only O(K log M) pilots vs. K pilots for classical methods, demonstrating that sparsity exploitation fundamentally improves the estimation-overhead trade-off. Third, CNN-DL attains 3–5 dB gain over OMP and 5–8 dB over MMSE, at the cost of substantial offline training data (10^5–10^6 samples) and distribution sensitivity. The DFT-thresholding estimator provides an excellent practical compromise: near-OMP performance at O(M log M) complexity via FFT.

IX. EMERGING CHALLENGES AND FUTURE RESEARCH DIRECTIONS

A. *Near-Field Estimation for XL-MIMO*

As arrays grow beyond M=1000, near-field (Fresnel) propagation dominates for nearby UEs. The planar wavefront assumption fails; the steering vector becomes a function of both angle and distance. Near-field channel estimation in polar-domain representations is an active open problem [31].

B. *RIS-Assisted Channel Estimation*

Reconfigurable intelligent surfaces (RIS) introduce cascaded BS–RIS–UE channels of dimension $M \times N^{DIL} \times K$ — vastly larger than conventional Massive MIMO. CS-based methods exploiting double sparsity and passive RIS-element switching protocols have shown promise, but prohibitive training overhead remains unsolved [32].

C. Grant-Free Access and Joint Activity Detection

For mMTC with sporadic transmissions, the BS must jointly perform activity detection and channel estimation. The active-device channel matrix is block-sparse. AMP with Bernoulli-Gaussian priors achieves near-optimal performance but scalability to millions of potential devices is still open [33].

D. Federated and Privacy-Preserving Channel Estimation

Federated learning enables multiple BSs to collaboratively train a shared estimation model without sharing raw CSI, preserving user privacy. Key challenges include gradient compression for communication efficiency and robustness to non-IID data distributions across cells [34].

E. Pilot Contamination Elimination

Beyond multi-cell MMSE, recent work shows pilot contamination can theoretically be eliminated via spatial covariance-based user grouping with specially designed non-orthogonal pilots and semi-blind estimation [35]. Practical implementation in dense heterogeneous networks remains an active frontier.

X. CONCLUSION

The paper has surveyed the estimation of channel with Massive MIMO systems on six paradigms: LS, MMSE, DFT/subspace, compressed sensing, angle-domain two-stage, and deep-learning. The main findings are: (i) LS is straightforward but noise-limited; (ii) MMSE is Bayes-optimal with O(M 3) cost; (iii) DFT-thresholding can achieve almost the same performance as MMSE with O(M log M) cost; (iv) CS/OMP can reduce pilot overhead by a factor of O(K log M) through sparsity exploitation; (v)

New channel estimation problems will be necessitated in future 6G systems with immensely large arrays, terahertz spectrums, RIS and massive IoT connectivity, and demand the convergence of electromagnetic theory, information theory, and current machine learning. It is an exciting research frontier that is built on this survey.

REFERENCES

[1] T. L. Marzetta, "Noncooperative cellular wireless with unlimited numbers of base station antennas," IEEE Trans. Wireless Commun., vol. 9, no. 11, pp. 3590–3600, Nov. 2010.
[2] [F. Rusek et al., "Scaling up MIMO: Opportunities and challenges with very large arrays," IEEE Signal Process. Mag., vol. 30, no. 1, pp. 40–60, Jan. 2013.
[3] E. G. Larsson, O. Edfors, F. Tufvesson, and T. L. Marzetta, "Massive MIMO for next generation wireless systems," IEEE Commun. Mag., vol. 52, no. 2, pp. 186–195, Feb. 2014.
[4] J. Hoydis, S. Ten Brink, and M. Debbah, "Massive MIMO in the UL/DL of cellular networks: How many antennas do we need?" IEEE J. Sel. Areas Commun., vol. 31, no. 2, pp. 160–171, Feb. 2013.
[5] Z. Jiang et al., "Achievable rates of FDD massive MIMO systems with spatial channel correlation," IEEE Trans. Wireless Commun., vol. 14, no. 5, pp. 2868–2882, May 2015.
[6] A. Alkhateeb et al., "Channel estimation and hybrid precoding for millimeter wave cellular systems," IEEE J. Sel. Topics Signal Process., vol. 8, no. 5, pp. 831–846, Oct. 2014.
[7] 3GPP TR 38.901, "Study on channel model for frequencies from 0.5 to 100 GHz," Release 16, v16.1.0, Jan. 2020.
[8] B. Hassibi and B. M. Hochwald, "How much training is needed in multiple-antenna wireless links?" IEEE Trans. Inf. Theory, vol. 49, no. 4, pp. 951–963, Apr. 2003.
[9] H. Yin et al., "A coordinated approach to channel estimation in large-scale multiple-antenna systems," IEEE J. Sel. Areas Commun., vol. 31, no. 2, pp. 264–273, Feb. 2013.
[10] A. Müller et al., "Efficient linear precoding for massive MIMO using truncated polynomial expansion," in Proc. IEEE SAM Workshop, pp. 273–276, Jun. 2014.
[11] E. Bjornson, J. Hoydis, and L. Sanguinetti, "Massive MIMO networks: Spectral, energy, and hardware efficiency," Found. Trends Signal Process., vol. 11, no. 3–4, pp. 154–655, Nov. 2017.
[12] C. Qi and L. Wu, "Uplink channel estimation for massive MIMO systems exploring joint channel sparsity," Electron. Lett., vol. 50, no. 23, pp. 1770–1772, Nov. 2014.
[13] W. Shen et al., "Channel feedback based on AoD-adaptive subspace codebook in FDD massive MIMO," IEEE Trans. Commun., vol. 66, no. 11, pp. 5235–5248, Nov. 2018.
[14] R. Couillet and M. Debbah, Random Matrix Methods for Wireless Communications. Cambridge University Press, 2011.
[15] S. Haghighatshoar and G. Caire, "Massive MIMO channel subspace estimation from low-dimensional projections," IEEE Trans. Signal Process., vol. 65, no. 2, pp. 303–318, Jan. 2017.
[16] D. L. Donoho, "Compressed sensing," IEEE Trans. Inf. Theory, vol. 52, no. 4, pp. 1289–1306, Apr. 2006.
[17] J. A. Tropp and A. C. Gilbert, "Signal recovery from random measurements via orthogonal matching pursuit," IEEE Trans. Inf. Theory, vol. 53, no. 12, pp. 4655–4666, Dec. 2007.

[18] J. Chen and X. Huo, "Theoretical results on sparse representations of multiple-measurement vectors," IEEE Trans. Signal Process., vol. 54, no. 12, pp. 4634–4643, Dec. 2006.
[19] R. Tibshirani, "Regression shrinkage and selection via the lasso," J. Roy. Statist. Soc. Ser. B, vol. 58, no. 1, pp. 267–288, 1996.
[20] D. L. Donoho, A. Maleki, and A. Montanari, "Message-passing algorithms for compressed sensing," Proc. Natl. Acad. Sci., vol. 106, no. 45, pp. 18914–18919, Nov. 2009.
[21] D. J. Love and R. W. Heath Jr., "Limited feedback unitary precoding for spatial multiplexing systems," IEEE Trans. Inf. Theory, vol. 51, no. 8, pp. 2967–2976, Aug. 2005.
[22] X. Rao and V. K. N. Lau, "Distributed compressive CSIT estimation and feedback for FDD multi-user massive MIMO," IEEE Trans. Signal Process., vol. 62, no. 12, pp. 3261–3271, Jun. 2014.
[23] A. Adhikary et al., "Joint spatial division and multiplexing—The large-scale array regime," IEEE Trans. Inf. Theory, vol. 59, no. 10, pp. 6441–6463, Oct. 2013.
[24] 3GPP TS 38.214, "NR; Physical layer procedures for data," Release 17, v17.4.0, Mar. 2023.
[25] T. Wang et al., "Deep learning for wireless physical layer: Opportunities and challenges," China Commun., vol. 14, no. 11, pp. 92–111, Nov. 2017.
[26] K. Zhang et al., "Beyond a Gaussian denoiser: Residual learning of deep CNN for image denoising," IEEE Trans. Image Process., vol. 26, no. 7, pp. 3142–3155, Jul. 2017.
[27] M. Soltani et al., "Deep learning-based channel estimation," IEEE Commun. Lett., vol. 23, no. 4, pp. 652–655, Apr. 2019.
[28] H. Ye, G. Y. Li, and B.-H. Juang, "Power of deep learning for channel estimation and signal detection in OFDM systems," IEEE Wireless Commun. Lett., vol. 7, no. 1, pp. 114–117, Feb. 2018.
[29] X. Liu et al., "Attention mechanism based neural network for channel estimation," in Proc. IEEE ICC, May 2022, pp. 1–6.
[30] V. Monga, Y. Li, and Y. C. Eldar, "Algorithm unrolling: Interpretable, efficient deep learning for signal and image processing," IEEE Signal Process. Mag., vol. 38, no. 2, pp. 18–44, Mar. 2021.
[31] M. Cui and L. Dai, "Channel estimation for extremely large-scale MIMO: Far-field or near-field?" IEEE Trans. Commun., vol. 70, no. 4, pp. 2663–2677, Apr. 2022.
[32] Z. He and X. Yuan, "Cascaded channel estimation for large intelligent metasurface assisted massive MIMO," IEEE Wireless Commun. Lett., vol. 9, no. 2, pp. 210–214, Feb. 2020.
[33] Z. Chen, F. Sohrabi, and W. Yu, "Sparse activity detection for massive connectivity," IEEE Trans. Signal Process., vol. 66, no. 7, pp. 1890–1904, Apr. 2018.
[34] B. McMahan et al., "Communication-efficient learning of deep networks from decentralized data," in Proc. AISTATS, Apr. 2017, pp. 1273–1282.
[35] R. R. Muller et al., "Blind pilot decontamination," IEEE J. Sel. Topics Signal Process., vol. 8, no. 5, pp. 773–786, Oct. 2014.

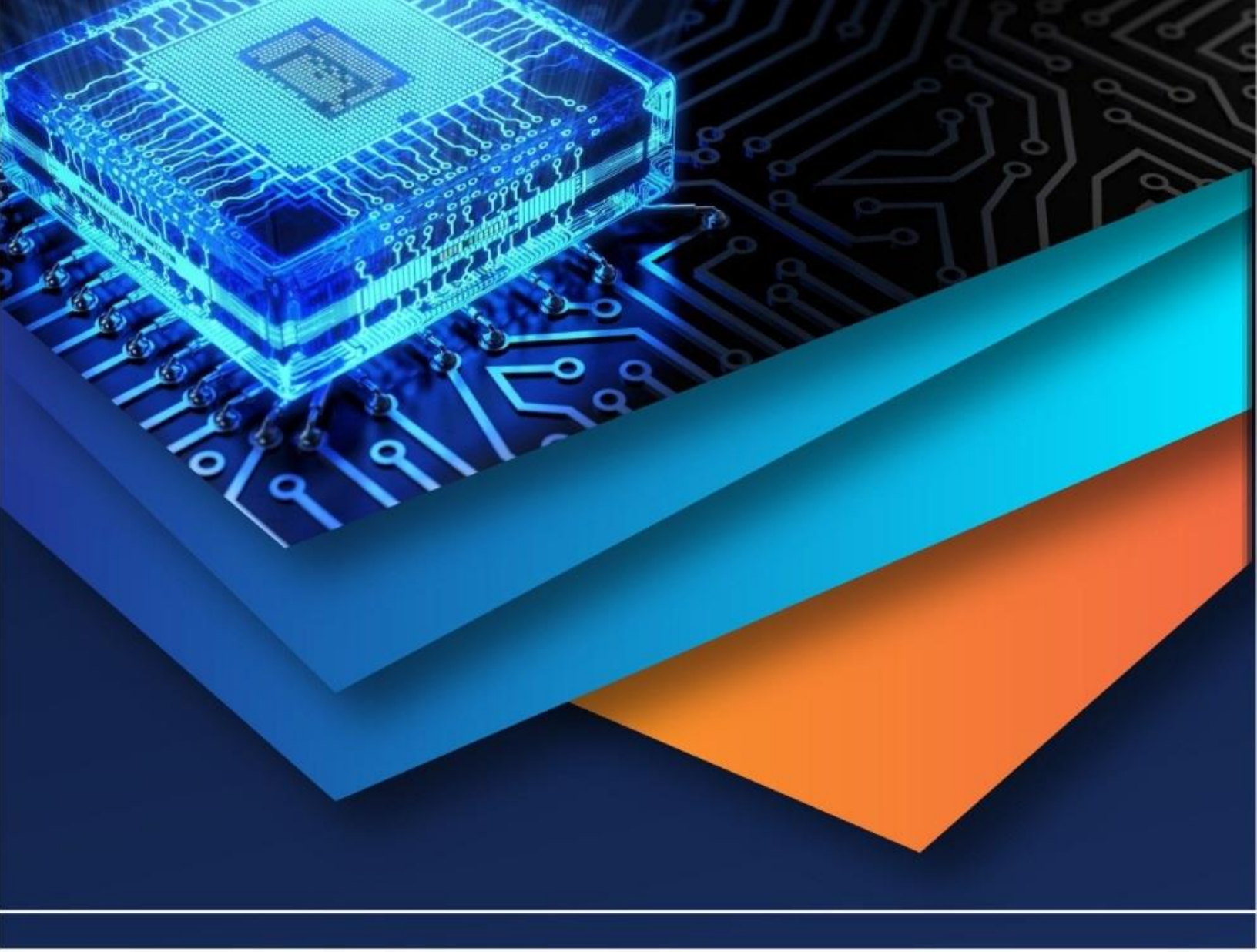

10.22214/IJRASET

45.98

IMPACT FACTOR: 7.129

IMPACT FACTOR: 7.429

INTERNATIONAL JOURNAL FOR RESEARCH

IN APPLIED SCIENCE & ENGINEERING TECHNOLOGY